LASER ALLOYED AL-NI-FE COATINGS

Paper (P115)

Sisa Pityana[1], Retha Rossouw[2]

[1] CSIR National Laser Centre, P. O Box 395, Pretoria 0001, South Africa

[2]National Metrology Institute of South Africa, Private Bag X34, Lynnwood Ridge, 004, South Africa

Abstract

The aim of this work was to produce crack-free thin surface layers consisting of binary (Al-Ni, Al-Fe) and ternary (Al-Ni-Fe) intermetallic phases by means of a high power laser beam. The laser surface alloying was carried out by melting Fe and Ni based powders on an aluminium substrate. The mixture of the Fe and Ni powders was varied in order to create Fe-rich and Ni-rich intermetallic phases. A Rofin 4.4 kW Nd: YAG laser was used for melting the powders and the substrate. The thin layers were analysed by means of X-ray diffraction (XRD), optical and scanning electron microscopy (SEM). It was found that when alloying with Fe-rich mixtures, the thin surface layers contained a number of cracks in the heat affected zones (HAZ). Alloying with Ni-rich mixtures produced crack-free surface layers on the substrate. The average thickness of the layer was ~1.5mm. The XRD analyses of the alloyed layer showed a variety of intermetallic phases including Ni_3Al, NiAl, FeAl, Fe_3Al and Al_5FeNi. The hardness of the surface layers was 3 ~ 4 times higher than that of the Al 1200 substrate.

Introduction

Among the techniques used for improving mechanical and chemical properties of the surface aluminium laser is surface alloying (LSA). The alloying technique can modify the chemical composition of the surface by incorporating alloying elements thus enhancing the wear and corrosion resistance. [1]. The process typically involves blowing an alloy powder into the laser created molten pool on the target surface. The critical processing parameters include laser power, laser beam spot size, scan speed and the powder feed rate.

LSA of aluminium with Ni, Fe and Mo has been reported previously [2-5]. The microstructure and X-ray diffraction of the alloyed aluminium revealed a presence of binary intermetallic phases of Al-Ni, Al-Fe and Mo-Al. These studies obtained great improvements of surface hardness in the region of 350 to 1000 HV.

The nickel and iron aluminides intermetallics are of particular importance and have received the most attention in recent studies [6-9]. They have good mechanical properties, excellent oxidation and corrosion resistance particularly at high temperatures. However, their lack of ductility has restricted their use. It has been shown recently that ductility of aluminides can be improved by adding small quantities of boron and thereby introducing disorder in the lattices [10].

The aims of the present work were to produce crack free thin layer surface alloys consisting of binary (Al-Ni, Al-Fe) and ternary (Al-Ni-Fe) intermetallics by means of high power laser treatment.

Experimental Procedure

Laser processing

The substrates used in the experiments were commercially pure AA1200 aluminium plates. The powder materials used for alloying were Fe and Ni with particle sizes ranging between 40 and 100 μm. The alloying powder was fed into the molten pool by means of an argon gas stream. A commercial powder feeder instrument equipped with a flow balance was used to control the powder feed rate. The argon gas flow rate was set at 2 L/min and the powder feed rate varied from 1 to 5 g/min. Figure 1 shows a schematic diagram of the experimental set-up.

Single tracks of Al-Ni-Fe laser alloyed samples were made on different substrates. The alloys were produced by mixing: (i) Fe and Ni powders in equal amounts and (ii) 60 wt % Ni and 40 wt % Fe.

A 4.4 kW Rofin Sinar Nd: YAG laser was used in the experimental investigation. The laser power was varied from 2.0 to 4.4 kW. The laser beam was focused onto the substrate surface to a spot size of 3.0 mm in diameter. A KUKA robot was used to deliver the laser beam to the target surface. The laser scan speeds were 8.0 mm/s, 10.0 mm/s and 12.0 mm/s.

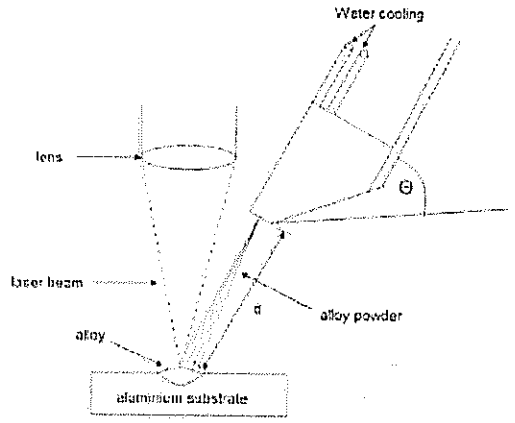

Figure 1 Schematic illustration of the laser alloying process.

Material Characterisation

Transverse and longitudinal sections of the alloyed specimen were prepared for structural, microstructural and micro-hardness investigation. The X-ray diffraction (XRD) patterns of the alloyed structures were obtained from polished sections using a PANaytical X' Pert Pro powder diffractometer with X' Celerator detector. The radiation sources used were Cobalt (Co Kα) and Copper (Cu Kα). The phases were identified using X' Pert High-score plus software.

The LEO 1525 scanning electron microscope (SEM) equipped with an energy dispersive spectrometer (EDS) was used for microstructure and elemental composition analysis. Optical microscope was also used for microstructure analysis. The hardness profiles of the alloyed samples were measured using a Matsuzawa hardness tester with a load of 100 g. A minimum of five indents were made in each location to obtain a good statistical representation of the dataset. In each case, the average of all the measurements was used to get the hardness profile of the alloyed track.

Results and Discussion

A number of experiments were performed at different laser power, scan speed and powder feed rate. When the laser power was set at 2.0 kW and scan speed varied from 8.0 to 10.0 mm/s there was no melt pool created on the surface. Some surface and powder melting was obtained at laser power of 3.0 kW and scan speeds of 8.0 and 10.0 mm/s. However, a very brittle non adherent thin layer was obtained. This layer was easily removed from the surface by mechanical brushing.

Successful laser alloys were obtained at laser power of 4.4 kW and scan speed of 10.0 mm/s. The powder feed rate which resulted in uniform and smooth alloyed zones were 1.0 and 3.0 g/min. There was insufficient mixing of the powder when the feed rate set at 5.0 g/min

Figure 2 shows a SEM micrograph of a cross-section of the layer formed with the 50 wt % Fe and 50 wt % Ni powders mixtures. The modified layer contains homogeneous lamella-like solidification dendrites. At the bottom of this layer isolated undissolved powder mixture can be seen. The depth of the modified layer was ~ 200 μm.

A detailed microstructure of the modified layer is shown in Figure 3. The microstructure of the modified layer is composed of a network of intermetallic compounds. The phases formed were identified by X-ray diffraction analysis (Figure 4). The identified phases are shown in Table 1. Some of the peaks could not be indexed due to strong overlap of the diffraction patterns of various intermetallic compounds.

The analysis shows that the surface contained a number of intermetallic phases of Al-Ni, Al-Fe and Al-Ni-Fe intermetallic compounds (Table 1). The intermetallic compounds are rich in both in Ni and Fe. The Al_5FeNi ternary compound was also identified. The dominant phases are rich in Al (Al_3Ni, Al_3Ni_2) and Ni (Ni_3Al). The formation of Ni rich intermetallics was also observed when the aluminium surface was laser alloyed with Ni powder alone. On the contrary the alloying of aluminium with Fe

powder produced very shallow, brittle thin layers which had cracks at the interface.

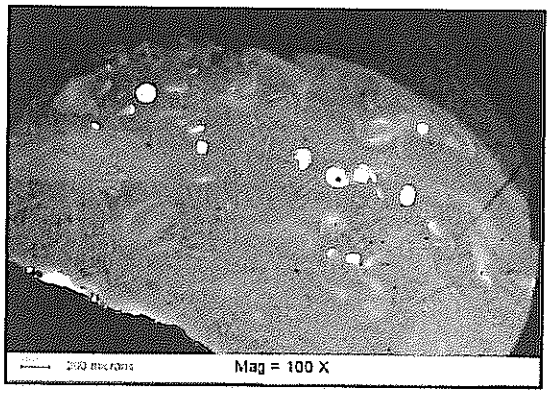

Figure 2 Cross-section of the 50 wt % Fe and 50 wt% Ni laser alloyed surface.

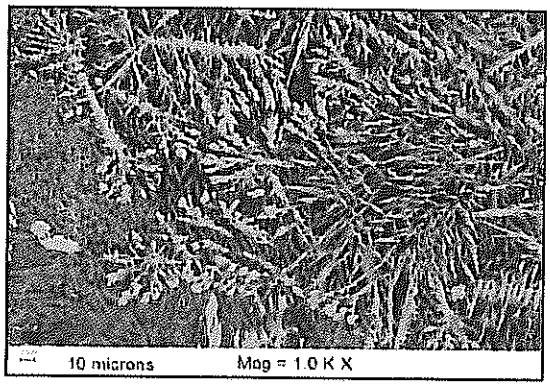

Figure 3 Microstructure of in the layer modified by 50 wt % Fe and 50 wt % Ni.

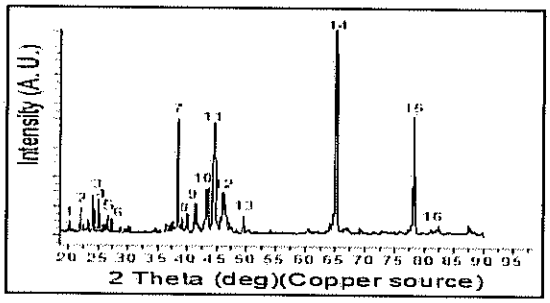

Figure 4 XRD spectrum of Al-Ni-Fe alloy obtained from the 50 wt % Fe and 50 wt % Ni powder mixtures.

Table 1 Phase identification of Al-Ni-Fe

S.No	2 Theta (deg)	Phase
1	20.11	$Al_{13}Fe_4$ (311)
2	22.03	Al_3Ni (011)
3	24.19	$AlNi_3$ (100)
4	25.09	
5	26.61	Fe_3Al (111)
6	38.47	α-Al (100)
7	40.07	-
8	41.49	Al_5FeNi (112)
9	43.59	AlFe (110)
10	43.85	$AlNi_3$ (111)
11	44.69	α-Al (200) Ni (111) A-Fe (110)
12	46.13	-
13	49.51	-
14	65.09	α-Al (220) α-Fe (200) Al_3Ni_2 (202)
15	78.17	Ni (220)

The micro-hardness profile of this modified layer is shown in Figure 5. The indentations were along the cross-section of the alloy. Hardness values as high as 1020 HV were measured on the thin layers resulting in improvement of the aluminium hardness.

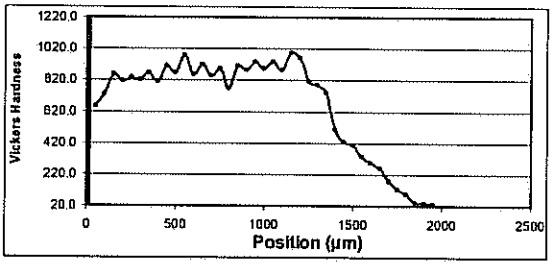

Figure 5 Micro-hardness profile of the Al-Fe-Ni alloyed obtained with 50 wt % Fe and 50 wt % Ni powders

Figures 6 shows a cross-section of the layer formed from the mixture of 60 wt % Ni and 40 wt % 50 Fe powders. The microstructure in the layer consists of dendrite and undissolved powder particles. Figure 7 shows a higher magnification of the alloyed layer.

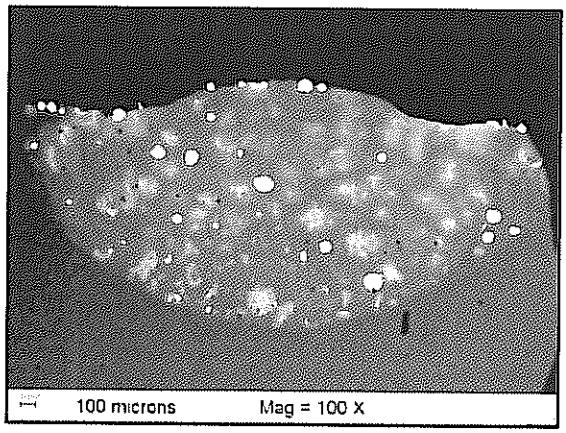

Figure 6 Cross section of 60 wt % Ni and 40 wt % Fe laser alloyed layer

The undissolved powder can be qualitatively explained in terms of convective mixing in the melt pool. The alloying powder has a higher specific gravities and melting temperatures compared to aluminium. The particles sink into the melt pool while at the same being carried along by the flow lines thus being distributed around the in alloyed layer. The molten aluminium solidifies before the alloying powder is dissolved; this leads to an alloyed layer consisting of a mixture of dendrites and undissolved power (Figure 7).

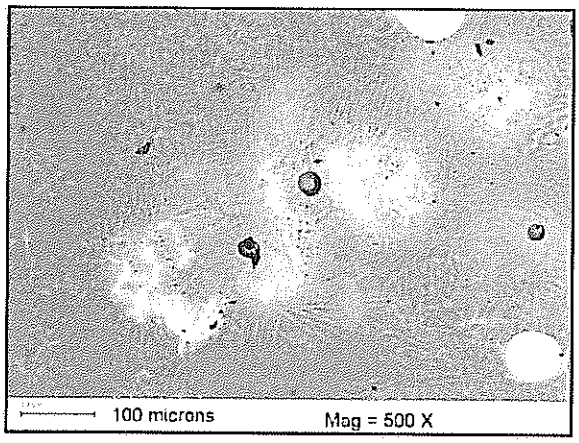

Figure 7 Microstructure of the 60% wt Ni and 40 wt % Fe powder mixture

X-ray diffraction analysis of the modified aluminium surface layer formed by mixing 60 wt % Ni and 40 wt % Fe was carried out with Co Kα target. The XRD spectrum is shown in Figure 8 and the phase identification is summarised in Table 2. The results indicate that the modified layer consist of binary intermetallics of Al-Fe, Al-Ni of various stoichiometries and ternary intermetallics Al-Fe-Ni.

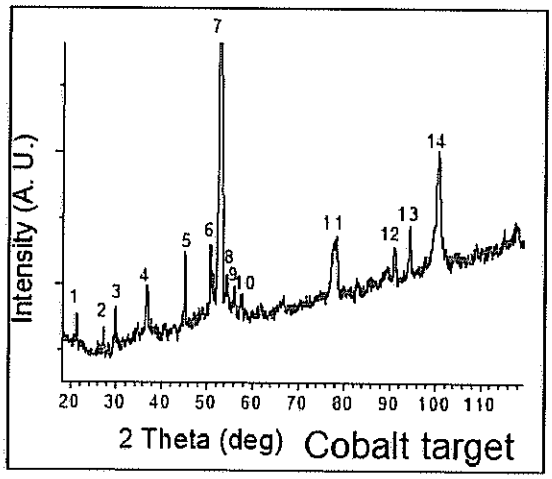

Figure 8 XRD spectrum of Al-Ni-Fe obtained from 60% wt Ni and 40 wt % Fe powder mixture

Table 2 Phase identification (Co Kα)

No	2 Theta (deg)	Phase
1	21.29	Al_3Ni_2 (001)
2	27.32	Al_5FeNi $Al3Fe_4$ (021)
3	29.90	Al_3Ni_2 (100)
4	36.86	$Al_{13}Fe_4$ Al_3Ni_2 (011)
5	45.11	Al (111)
6	50.72	$AlFe_3$ Al_5FeNi
7	52.64	α-Al(200) Ni(200) AlFe(110) α-Fe(110) Al_3Ni_2
8	56.10	Al_3Ni (212)
9	57.55	Al_3Ni_2
10	58.20	Al_5FeNi
11	78.21	α-Fe(200) α-Al(220)
12	90.88	$AlNi_3$ (220)
13	94.38	α-Al (311) Ni (220)
14	100.62	α-Al (222) Al_3Ni_2 (122)

The Vickers microhardness profile measured along the cross-section of the alloyed layer is shown in Figure 9. The average hardness measured was 1020 HV. This high hardness results from the high volume fraction of the intermetallics in the alloyed layer.

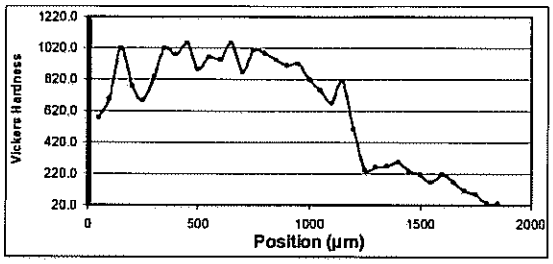

Figure 9 Micro-hardness profile of Al-Fe-Ni alloy obtained with 60 wt % Ni and 40 wt % Ni powder mixtures

Conclusions

Laser surface alloying of aluminium was carried out by varying the composition of the Ni and Fe powder mixtures. A crack free alloyed layer with very high hardness value was obtained on the aluminium substrate. Very high hardness values ~ 1020 HV were obtained for high nickel content powders, however, a very high concentration of undissolved powders were trapped in the solid solution. The hardness of the layers was 3 to 4 times higher than that of the base material.

The X-ray diffraction results showed thin layers consisting of various intermetallic phases consisting of Ni_3Al, NiAl, FeAl and Fe_3Al. The ternary Al_5FeNi was also obtained in the laser formed by mixing nickel and iron powders.

References

[1] M. H. Sohi, J. Materials Processing Technology, **118**, (2001) 187

[2] S. Bysakh, et al, Metallurgical and Materials Trans., **34A**, (2003), 2621

[3] E. Gaffet, J. M. Pelletier and S. Bonnet-Jobez, Acta Metall., **37**, (1989), 3205

[4] L. G. Jonnes and A. Olsen, J. Materials Science, **29**, (1994), 728

[5] Y. Y. Qiu, A. Almeida and R. Vilar, J. Materials Science, **33**, (1998) 2639

[6] G. Temizel and M. Özenbaş, Turkish J. Eng. Envi. Sci, **31**, (2007), 71

[7] Q. Zeng and I. Baker, Intermetallics, **14**, (2006), 396

[8] W. Maziarz, J. Dutkiewicz and J. Senderski, J. Mat. Sci, **39**, (2004), 5425

[9] L. Eleno, K. Frisk and A. Schneider, Intermetallics, **14**, (2006), 1276,1

[10] U. K. kattner, T. B. Massalski, 'Binary Alloy Phase Diagrams", H. Baker (Ed), ASM International, Material Park, (1990)

Acknowledgements

The authors thank Mr Chris Kruger and Mr Herman Burger for helping with the operation of the laser. We also acknowledge financial support from the CSIR-NLC.